

Robust soliton clusters in media with competing cubic and quintic nonlinearitiesD. Mihalache,^{1,2,3} D. Mazilu,^{2,3} L.-C. Crasovan,¹ B. A. Malomed,⁴ F. Lederer,³ and L. Torner¹¹*ICFO-Institut de Ciències Fòtiques, and Department of Signal Theory and Communications, Universitat Politècnica de Catalunya, ES 8034 Barcelona, Spain*²*Department of Theoretical Physics, Institute of Atomic Physics, P.O. Box MG-6, Bucharest, Romania*³*Institute of Solid State Theory and Theoretical Optics, Friedrich-Schiller Universität Jena, Max-Wien-Platz 1, D-07743 Jena, Germany*⁴*Department of Interdisciplinary Studies, Faculty of Engineering, Tel Aviv University, Tel Aviv 69978, Israel*

(Received 6 May 2003; published 27 October 2003)

Systematic results are reported for dynamics of circular patterns (“necklaces”), composed of fundamental solitons and carrying orbital angular momentum, in the two-dimensional model, which describes the propagation of light beams in bulk media combining self-focusing cubic and self-defocusing quintic nonlinearities. Semianalytical predictions for the existence of quasistable necklace structures are obtained on the basis of an effective interaction potential. Then, direct simulations are run. In the case when the initial pattern is far from an equilibrium size predicted by the potential, it cannot maintain its shape. However, a necklace with the initial shape close to the predicted equilibrium survives very long evolution, featuring persistent oscillations. The quasistable evolution is not essentially disturbed by a large noise component added to the initial configuration. Basic conclusions concerning the necklace dynamics in this model are qualitatively the same as in a recently studied one which combines quadratic and self-defocusing cubic nonlinearities. Thus, we infer that a combination of competing self-focusing and self-defocusing nonlinearities enhances the robustness not only of vortex solitons but also of vorticity-carrying necklace patterns.

DOI: 10.1103/PhysRevE.68.046612

PACS number(s): 42.65.Tg

I. INTRODUCTION

Optical solitons, that is, self-supporting localized light pulses and beams, have been predicted and observed in various physical settings over the last three decades [1–3]. They appear as one-dimensional (1D) temporal solitons in nonlinear fibers, 1D and two-dimensional (2D) spatial solitons (self-localized light beams) in planar and bulk waveguides, and three-dimensional 3D spatiotemporal solitons (alias “light bullets” [4]) in bulk optical media. The “bullets” are completely localized traveling pulses of light, their 2D counterparts being possible too as spatiotemporal solitons in planar waveguides (in fact, the only species of the light bullets that were thus far created in a real experiment were quasi-2D solitons in bulk samples [5]). Recently, interest in this area has been extended to the study of complex soliton structures composed of several interacting solitons in the form of necklace-ring beams [6,7] in self-focusing nonlinear media.

The existence of spiraling self-localized structures in Hamiltonian systems described by the cubic nonlinear Schrödinger (NLS) equations was analyzed in Ref. [8]. Later, a rigorous criterion for the stability of solitary-wave structures in Hamiltonian systems carrying orbital angular momentum was reported [9], which is applicable to stationary structures with a broken rotational symmetry.

Two-dimensional soliton clusters in saturable self-focusing media, which were recently introduced in Ref. [10], are ring-like soliton complexes in bulk media, having a staircase-like phase distribution that induces a nonzero orbital angular momentum leading to rotation of the cluster. They are generally metastable (i.e., in the absence of any perturbations they can propagate stably over many diffraction lengths in the saturable medium), eventually experiencing a symmetry-breaking instability. However, initial pertur-

bations destabilize the cluster after passing only a few diffraction lengths, and it eventually disintegrates into a set of isolated 2D solitons. Soliton clusters in two and three dimensions, respectively, may be viewed as a nontrivial generalization of the 2D bright or dark vortex solitons [11–16], and 3D “spinning” solitons (vortex tori) [17–19]. The concept of soliton clusters has been also introduced in the study of non-Hamiltonian nonlinear systems such as externally driven optical cavities [20]. In such systems, the simplest example is a two-dimensional clustered pattern observed in the transverse plane [20].

These new concepts of complex soliton structures may apply to other nonlinear physical media, including the prediction of Skyrmions [21] in a two-component Bose-Einstein condensate (BEC) [22] (for a recent comprehensive review of BEC of atomic gases in a trap, see, for example, Ref. [23]). We mention recent progress in the generation of topological states (vortices) carrying different angular momenta [24] in a two-component BEC [25] and in a stirred BEC [26], the observation of a regular triangular vortex lattice in rotating BECs [27], formation and propagation of bright matter-wave solitons trains in a quasi-1D optical trap [28], the theoretical prediction that a matter-wave bright soliton can be stabilized in 2D geometries by causing the nonlinearity strength to rapidly oscillate between positive and negative values (through the Feshbach resonance) [29,30]; still earlier works on vortices and solitons in BECs were reviewed in Ref. [31]. Closely related topics are the recently introduced concepts of globally linked vortex clusters in nonrotating BEC with attractive interactions [32], of ring dark solitons and vortex necklaces in BECs [33], and of soliton “molecules” in optics and hybrid atomic-molecular BECs [34,35]. The soliton-cluster concept is also relevant to the field of mixed atomic-molecular BECs [36–43].

In media with pure quadratic or cubic nonlinearity, soliton clusters always tend to self-destroy through expansion or collapse, or, at best, they exist as metastable states which are broken up too by small perturbations [6,7,10,44–47]. In the presence of two competing optical nonlinearities (self-focusing and self-defocusing ones), the instability may be greatly weakened, and the soliton complexes may propagate stably over huge distances even in the presence of random perturbations. The first example of the formation of both 2D and 3D robust soliton clusters was put forward in the case of competing quadratic and cubic nonlinearities; these soliton complexes are multicolored, they carry nonzero orbital angular momentum and are linked via a staircase-like phase distribution [34,48]. A fact which helps to understand the stabilization of these clusters is the existence of *completely stable* 2D bright vortex solitons [49] and 3D stable vortex tori [19] in the same media; intuitively, the clusters may thus be considered as fragmented counterparts of these stable objects.

Recently, it was shown that similar stable bright 2D and 3D spinning solitons, carrying nonzero orbital angular momentum, also exist in media with competing cubic and quintic nonlinearities [50–54,18], which suggests searching for quasistable soliton clusters in the multidimensional NLS models with the competing self-focusing cubic and self-defocusing quintic nonlinearities. A purport of such an investigation is to understand whether the stabilized clusters are generic objects, by comparing their basic properties in the quadratic-cubic and cubic-quintic (CQ) models (this way, it has been demonstrated that the above-mentioned stable “spinning” solitons are generic indeed, in both 2D and 3D cases). Besides that, the investigation of the clusters in the CQ medium expands possibilities for experimental creation of such structures. In this context, it is worth noticing that it was recently suggested that dielectric response of several different media may be modeled by the CQ nonlinearity, accompanied by significant two-photon absorption [55]. The objective of this work is the search for quasistable soliton clusters in the 2D model with the CQ nonlinearity.

The rest of the paper is organized as follows. In Sec. II, 2D necklace-like soliton complexes in the CQ medium are constructed. Direct numerical simulations of their propagation, which proves that they are quasistable indeed, are presented in Sec. III. The results of the work are summarized in the concluding section.

II. CONSTRUCTION OF TWO-DIMENSIONAL SOLITON CLUSTERS IN CUBIC-QUINTIC MEDIA

The equation governing the evolution of the field is a modified NLS equation of the CQ type, written in a normalized form

$$iu_Z + u_{XX} + u_{YY} + |u|^2 u - \alpha |u|^4 u = 0, \quad (1)$$

where α is a parameter which characterizes the strength of the quintic nonlinearity that can be scaled out from this equation (see below). This generic model, in its 1D and multidimensional variants, appears in various branches of nonlinear science; for earlier work on this issue in the context of nonlinear optics, see, for example, Ref. [56]. In the most typical

case, Eq. (1) governs the spatial evolution of the time-independent complex amplitude of the electromagnetic wave along the axis Z in a bulk medium with transverse coordinates X and Y ; soliton solutions to be found in this case then represent spatial solitons, i.e., self-trapped light beams in the bulk medium.

Before proceeding to the necklace patterns, we revisit the recently investigated problem of constructing spinning-soliton solutions to Eq. (1). To this end, stationary solutions are looked for in the form

$$u = U(r) \exp(iS\theta) \exp(i\kappa Z), \quad (2)$$

where r and θ are the polar coordinates in the (X, Y) plane, κ is the wave number (the propagation constant), and the integer S is the topological charge of the soliton (which is sometimes called “spin”). Waveform (2) exhibits nonzero z component of the orbital angular momentum (see below) if $S \neq 0$.

The amplitude U may be assumed real, and it then obeys an equation

$$U'' + r^{-1}U' - S^2 r^{-2}U - \kappa U + U^3 - \alpha U^5 = 0, \quad (3)$$

where the wave number κ parametrizes the family of stationary solutions.

Equation (1) conserves a dynamical invariant, which has the meaning of the net power of the light beam:

$$E = \int_{-\infty}^{\infty} \int_{-\infty}^{\infty} |u(X, Y)|^2 dX dY. \quad (4)$$

Another dynamical invariants are the Hamiltonian,

$$H = \int_{-\infty}^{\infty} \int_{-\infty}^{\infty} [|u_X|^2 + |u_Y|^2 - (1/2)|u|^4 + (1/3)\alpha |u|^6] dX dY, \quad (5)$$

momentum (equal to zero for the solutions considered in this work) and the z component of the angular momentum,

$$L_z = \int_{-\infty}^{\infty} \int_{-\infty}^{\infty} (\partial\phi/\partial\theta) |u|^2 dX dY, \quad (6)$$

ϕ being the phase of the complex field u . Using Eq. (3), one can readily find that $L_z = SE$, and

$$H = -(2\pi/3)\alpha \int_0^{\infty} U^6(r) r dr. \quad (7)$$

Notice that the parameter α can be rescaled, $\alpha \rightarrow \tilde{\alpha} \equiv \lambda \alpha$ (λ is an arbitrary positive scaling factor), by defining $\tilde{Z} = \lambda Z$, $\tilde{X} = \lambda^{1/2} X$, $\tilde{Y} = \lambda^{1/2} Y$, $\tilde{U} = \lambda^{-1/2} U$. This leads to the corresponding scaling of κ , E , and H :

$$\tilde{\kappa} = \kappa/\lambda; \quad \tilde{E} = E; \quad \tilde{H} = H/\lambda.$$

The existence region for the 2D solitons that are sought for in form (2) is $0 < \kappa < \kappa_{\text{offset}}^{(2D)} \approx 0.18/\alpha$, regardless the value of the topological charge (spin) [50,57]. Note that a soliton so-

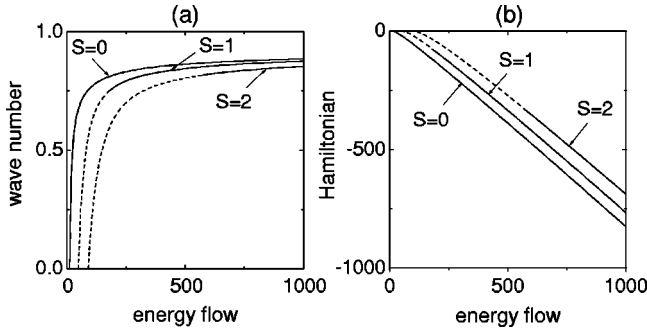


FIG. 1. The propagation constant κ (a) and Hamiltonian H (b) of the two-dimensional solitons vs the power E . Here and below, the scaling factor α in front of the cubic term in Eq. (1) is fixed to be 0.2.

lution to the 1D version of Eq. (1) is known in an exact form, the corresponding offset wave number being $\kappa_{\text{offset}}^{(1D)} = 3/(16\alpha) \equiv 0.1875/\alpha$, so that the above value of $\kappa_{\text{offset}}^{(2D)}$ is quite close to it (see Ref. [57]). Throughout this work, we fix $\alpha = 0.2$.

One-parameter families of the 2D spinning solutions can be found in a numerical form. The solitons have the form of a ring vortex with a hole in the center (since the field must vanish $\sim r^{|S|}$ as $r \rightarrow 0$). In accordance with the results predicted by means of the semi-analytical variational approximation developed in Ref. [50] (see also Ref. [57]), the solutions exist provided that their energy exceeds a certain threshold value. As a test for the accuracy of numerical computations, we used a relationship which can be obtained directly from Eq. (3):

$$\kappa E = \pi \int_0^\infty r U^4(r) dr - (2\pi/3)\alpha \int_0^\infty U^6(r) r dr. \quad (8)$$

To quantify the 2D solitons, in Fig. 1 we show the nonlinear wave number κ and the Hamiltonian H for the solitons with topological charge $S=0$, $S=1$, and $S=2$ versus their power E . In the figure, continuous and dashed lines correspond to branches that, respectively, have been found to be stable and unstable [52–54]. Moreover, a recent work [53], which was carried out by means of very accurate numerical methods applied to the computation of stability eigenvalues, has shown the existence of *stable* 2D spinning solitons with higher (>2) values of S in the CQ model, the width of the stability region decaying with S according to an empirically found law, const/S^2 . Note that κ corresponding to the vortex solution monotonously increases with E , showing saturation (to the above-mentioned limiting value $\kappa_{\text{offset}}^{(2D)}$), at large val-

ues of E . It is also relevant to mention that the minimum energy necessary for the existence of the soliton drastically increases with S . Numerically, exact values of the threshold are $E_{\text{thr}} = 11.734$, 48.379, and 88.338 for $S=0$, 1, and 2, respectively.

In fact, all the results for the stationary spinning solitons in the present model were already obtained in previous works, see above. The nonlinear states that we investigate in what follows are circular soliton necklaces, which we constructed starting with a superposition of N fundamental (non-spinning) solitons set along a circumference of some radius R_0 , with a fixed phase difference between adjacent ones, so that the overall phase change along the circumference is $2\pi M$, where M is the net topological charge of the soliton complex [10]. Thus, the initial ansatz is

$$u(Z=0) = \sum_{n=1}^N U_0(|\vec{r} - \vec{r}_n|) e^{i\phi_n}, \quad (9)$$

where U_0 is the stationary fundamental ($S=0$) soliton, \vec{r}_n are positions of the soliton centers chosen as specified above, and the soliton phases at these points are $\phi_n = 2n\pi M/N$. The parameters that control the dynamics of the soliton clusters are the topological charge M , the number of “beads” N forming the “necklace,” its initial radius R_0 , and the power E of each constituent soliton.

Note that ansatz (9) implies that the phase distribution in the initial cluster has the shape of a staircase. Below, we will also consider another possibility, with a continuous initial phase distribution that has a form of a ramp with a constant slope,

$$u(Z=0) = \sum_{n=1}^N U_0(|\vec{r} - \vec{r}_n|) e^{iM\theta}, \quad (10)$$

where M is, as above, the net vorticity, and θ is the angular coordinate in the (X, Y) plane.

Recall that the vortex solitons are stable in the present model if their power exceeds a threshold value [52–54]. We therefore focused on the study of clusters whose initial total power exceeds the corresponding stability-threshold value of the vortex soliton, in anticipation that, for smaller values of the net power, the necklaces have no chance to be stable. Because the stability threshold for the $S=1$ vortex soliton at $\alpha=0.2$ is $E_{\text{thr}} \approx 180$ (see Fig. 1), we have considered, for instance, the clusters with net topological charge $M=1$, composed of $N=4, 5$, and 6 fundamental solitons, each hav-

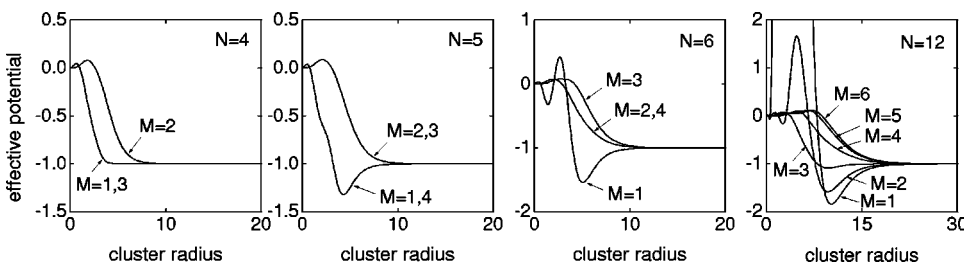


FIG. 2. The effective interaction potential vs the radius for the necklaces composed of $N=4$, 5, 6, and 12 solitons, at different values of the vorticity carried by the pattern.

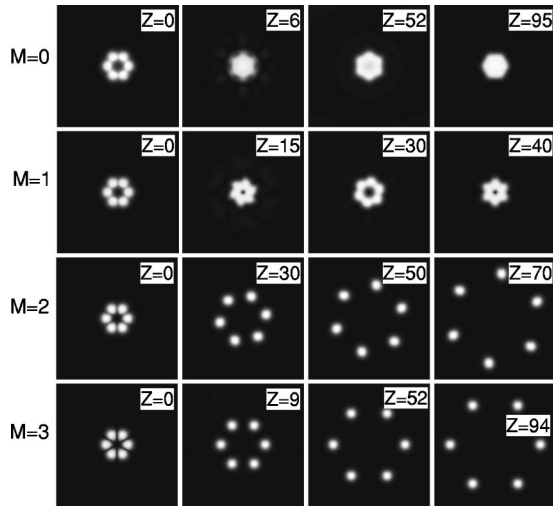


FIG. 3. Propagation regimes of the soliton clusters with $N=6$ and different values of the net vorticity M (in the absence of noise). All the clusters in this plot and in the following ones are built up of solitons with the power $E=80$.

ing the power $E=80$, so that the net power of the cluster is well within the stability region of the vortex soliton with the topological charge $S=1$.

For ansatz (9), the cluster's interaction Hamiltonian (alias the effective potential of the interaction), defined as $H(R_0)/|H(R_0=\infty)|$, was numerically computed as a function of R_0 and M [recall the Hamiltonian is defined in Eq. (5)]. This quantity gives important clues concerning the existence and stability of bound states of solitons (see Refs. [58] and [10]). The result is that, for the cluster with $N=4$ constituents, the interaction Hamiltonian does not have any minimum for any M (see Fig. 2), but for $N=5$, $N=6$, and $N=12$, local minima of the Hamiltonian are found for $M=1$ (as well as for some other values of M), which suggests the existence of quasistable necklace patterns in these cases.

III. ROBUSTNESS OF THE SOLITON CLUSTERS IN THE CUBIC-QUINTIC MEDIUM

In order to check the predictions following from the computation of the effective potential, we directly simulated Eqs.

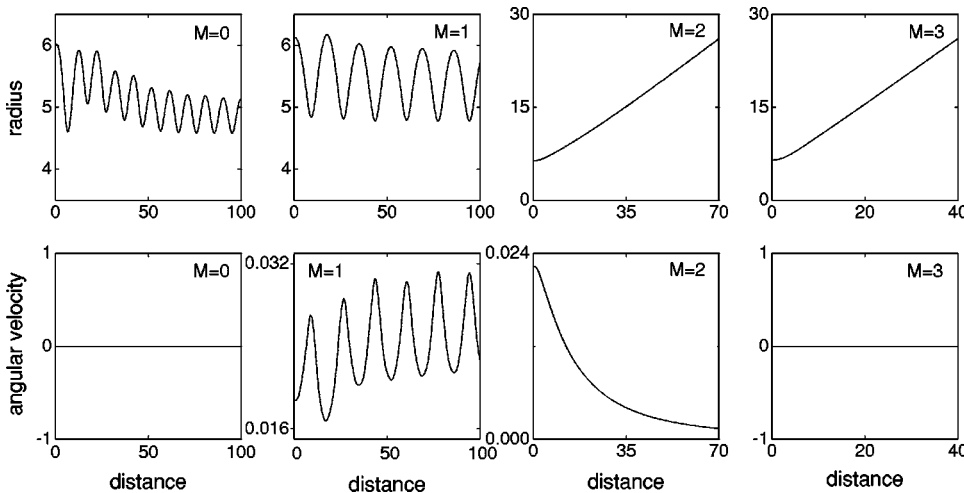


FIG. 4. The evolution of the cluster's mean radius (top row) and mean angular velocity (bottom row) for different values of the vorticity M . Parameters are same as in Fig. 3.

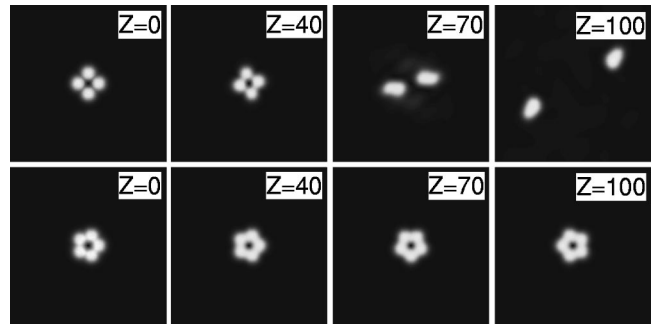


FIG. 5. Breakup of a cluster composed of four solitons under the action of random noise (top row), and robust evolution of a cluster composed of five solitons (bottom row). In both cases, $M=1$ and $R_0=4.5$.

(1) by means of a finite-difference scheme based on the Crank-Nicholson method, followed by the Newton-Picard iterative technique and the Gauss-Seidel method for solving the resulting linear system of equations. To achieve good convergence, we needed, typically, five Picard iterations and eight Gauss-Seidel iterations. In most cases, we employed the transverse-grid stepsize $\Delta X = \Delta Y = 0.3$ and the longitudinal stepsize $\Delta Z = 0.003$. Transparent boundary conditions allowing the radiation to escape from the computation window were implemented, to prevent possible artificial effects caused by radiation waves reentering the integration domain.

The evolution of the cluster's mean radius $R(Z)$ and of the cluster's mean angular velocity $\omega(Z)$ was monitored. These quantities were defined as follows:

$$R(Z) \equiv E^{-1} \int_{-\infty}^{\infty} \int_{-\infty}^{\infty} (X^2 + Y^2)^{1/2} |u|^2 dXdY \quad (11)$$

and

$$\omega(Z) \equiv L_z / I, I \equiv \int_{-\infty}^{\infty} \int_{-\infty}^{\infty} (X^2 + Y^2) |u|^2 dXdY, \quad (12)$$

where L_z is the z component of the angular momentum, see Eq. (6), and I is the cluster's moment of inertia. Because the

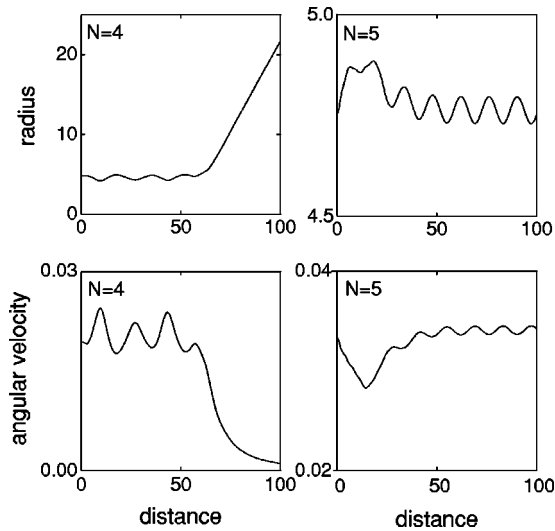


FIG. 6. The evolution of the mean radius (top row) and angular velocity (bottom row) in the clusters composed of four and five solitons. Parameters are same as in Fig. 5.

initial radius R_0 of the cluster is large, it is easy to see that the initial value of the average radius (11) amounts to $R(0) \approx R_0$.

Keeping $M=1$, we varied the initial cluster's radius R_0 around the minimum value predicted by the effective potential in Fig. 2. In this way, a range of optimum values of R_0 was found that minimize oscillations of the mean radius in the course of the propagation (z evolution), which implies that the cluster is a nearly stationary state. For $N=6$, the optimum values are close to $R_0=6$, whereas for $N=5$, it is $R_0=4.5$. In Figs. 3 and 4 we show typical examples of the evolution of the clusters composed of $N=6$ beads. These necklace clusters are nonstationary: they gradually fuse or expand and rotate during the evolution.

In the special case $M=nN$ ($n=0,1,2,\dots$) the cluster actually has zero angular momentum, as the phase shifts between adjacent beads is a multiple of 2π , so it is tantamount to being zero; in this case, the solitons attract each other and the cluster fuses into a single fundamental (nonspinning)

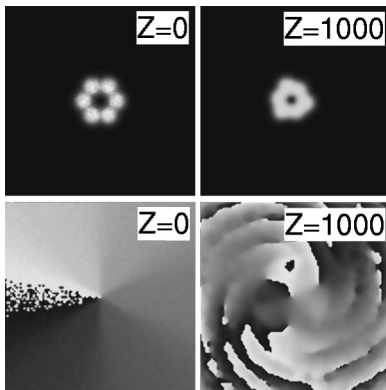


FIG. 7. Evolution of the cluster over long distance in the presence of input noise. The net vorticity is $M=1$, the input radius is $R_0=6$, and the phase distribution in the initial cluster is in the form of the staircase.

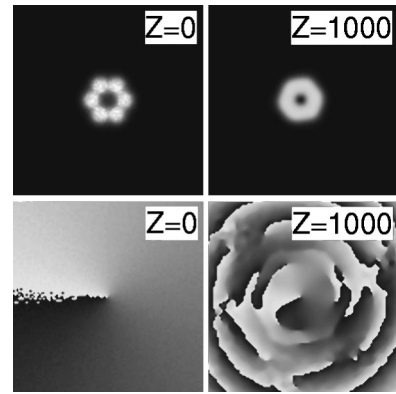


FIG. 8. Same as in Fig. 7, but with the continuous ramp-like phase distribution at the input.

soliton (see the first row in Fig. 3 and the first column in Fig. 4, corresponding to $N=6$ and $M=0$).

The cluster actually has zero angular momentum also for even N and $M=(2n+1)N/2$ ($n=0,1,2,\dots$). However, in this case the phase difference between adjacent beads is π times an odd integer, hence the interaction between the solitons is repulsive (see Fig. 2). Therefore, the clusters gradually expand in this case (see the fourth row in Fig. 3 and the fourth column in Fig. 4, corresponding to $N=6$ and $M=3$).

When $N=6$ and $M=2$, the cluster has a true nonzero angular momentum and the propagation shows gradual expansion and rotation (see Figs. 3 and 4). When $M=1$ and $N=6$, the potential is attractive (see Fig. 2), however the nonzero net angular momentum of the structure prevents fusion of the beads. In such cases, generic behavior is quasiperiodic expansion and shrinking of the cluster, which persists over tens of diffraction lengths, as is shown in the second row in Fig. 3 and the second column in Fig. 4. The latter case may be naturally categorized as a truly robust one.

To further study the cluster's robustness, we ran numerical experiments, adding random noise to the input field con-

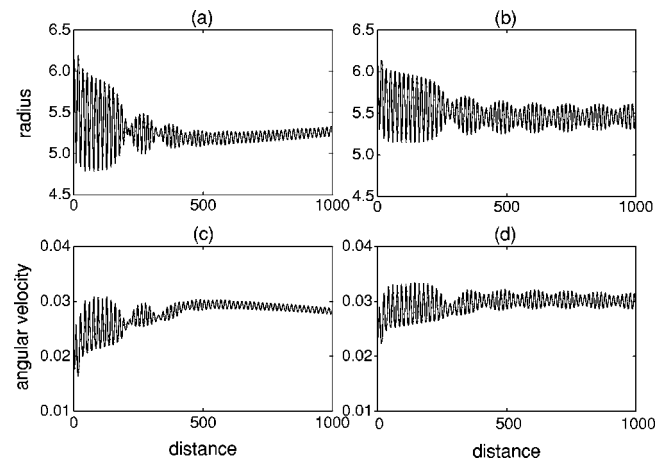


FIG. 9. The evolution of the mean radius (top row) and angular velocity (bottom row) for the clusters composed of six solitons, with the input radius $R_0=6$. In (a) and (c), the initial staircase-like phase distribution was used, whereas in (b) and (d) it was the ramp-like distribution.

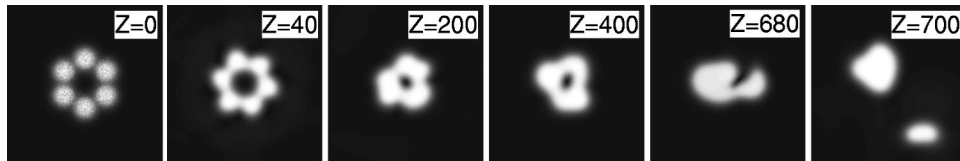


FIG. 10. The evolution of clusters composed of six solitons in the presence of random input noise. Here, the net vorticity is $M=1$ and the input radius is $R_0=7$. The initial phase distribution is the staircase-like one.

figuration (9) in two distinct ways: (i) multiplying it by $[1 + \rho(X, Y)]$, where ρ is a Gaussian random function with some variance σ (usually we took $\sigma=0.1$) and zero mean value, or (ii) multiplying it by $[1 + \epsilon(\rho_1 + i\rho_2)]$, where $\rho_{1,2}$ are uniformly distributed random numbers in the interval $[-0.5, 0.5]$ (usually we took $0.05 \leq \epsilon \leq 0.2$). Typical examples of the evolution of the perturbed clusters composed of 4 and 5 solitons are shown in Figs. 5 and 6. In these examples, uniformly distributed noise with a moderate amplitude $\epsilon=0.05$ was added. The clusters composed of four solitons do not survive the disturbed propagation over 100 diffraction lengths (they eventually break up into two separate fragments), whereas clusters with $N=5$ show a remarkable robustness over this and longer propagation distance.

We also compared the long-scale evolution of the clusters perturbed by the random noise in the cases when the phase mask, created by the initial phase distribution, had the staircase and ramp shapes, see Eqs. (9) and (10), and the propagation distance was extremely large. The results are displayed, for the staircase and ramp profiles and identical initial intensity distributions, in Figs. 7 and 8, respectively. Note that, in both cases, not only the propagation distances are very large, but also the uniformly distributed input noise has a large amplitude, $\epsilon=0.2$. We take $N=6$, $M=1$, and the input radius $R_0=6$, a value slightly larger than that corresponding to the minimum of the interaction Hamiltonian in this case (see Fig. 2). In both cases, the clusters show a trend to *slow fusion* into a quasiuniform ring, i.e., a stable vortex soliton, with the same value of the vorticity ($S=1$, in the cases shown in Figs. 7 and 8) which the original cluster was given. The eventual fusion into the single vortex soliton sets a limit for the robustness of the momentum-carrying clusters. Figure 9 additionally shows comparison of the evolution of the cluster's mean radius and angular velocity for the same two inputs. In both cases, we see quasiperiodic evolution of the soliton complex.

Further, in Fig. 10 we display the case when the initial cluster's radius was increased from $R_0=6$ to $R_0=7$ (in this case, only the cluster with the initial staircase-like phase distribution is shown). As is seen, the cluster survives about 50 diffraction lengths under the action of the input Gaussian noise (with the variance $\sigma=0.1$). However, the difference from the situation shown in Figs. 7–9 is that, in the present case, the initial separation between the solitons forming the cluster is farther from that which corresponds to the equilibrium value predicted by the effective interaction Hamiltonian. This difference turns out to be essential: the soliton complex cannot eventually merge into a quasiuniform ring; instead, it yields to the self-demolition azimuthal instability, see Fig. 10.

Thus, the value of the cluster's initial radius is a crucially important parameter which determines its subsequent evolution. We have found that in the case of the cluster composed of closely packed $N=6$ fundamental solitons having the net vorticity $M=1$, with the initial radius $R_0=6$, the output field pattern is a stable vortex ring with the topological charge $S=1$, even if the input phase was a staircase-like one (see Figs. 7 and 9). However, if the initial radius is increased to $R_0=7$, the input field distribution is far from that corresponding to the stable $S=1$ vortex ring, and the cluster eventually disintegrates into several fragments (see Fig. 10 for the typical evolution over long distances in this case).

IV. CONCLUSION

In this work, we have developed systematic dynamical analysis of circular patterns, built up of fundamental solitons and carrying angular momentum, in the 2D cubic-quintic model. Predictions for the existence of quasistable necklace structures were made in a semianalytical form, using the effective interaction potential. Then, direct simulations have shown that, in the case when the initial pattern is far from an equilibrium configuration predicted by the potential, it quickly collapses into a single zero-vorticity soliton, or decays into a set of noninteracting solitons. However, if the necklace is sufficiently close to a predicted equilibrium, it survives in the course of very long evolution, demonstrating persistent oscillations around the equilibrium configuration. This character of the evolution is not essentially disturbed by adding a large noise component to the initial condition.

The basic conclusions concerning the necklace dynamics in this model are qualitatively the same as in a recently considered model combining quadratic and self-defocusing cubic nonlinearities. This makes it possible to infer that a combination of competing self-focusing and self-defocusing nonlinearities stabilizes not only vortex solitons but also vorticity-carrying circular multisoliton arrays.

ACKNOWLEDGMENTS

Support from the Institució Catalana de Recerca i Estudis Avançats (ICREA), Spain, the Spanish government through Contract No. BFM2002-2861, and Deutsche Forschungsgemeinschaft (DFG), Germany, is acknowledged. B.A.M. appreciates hospitality of the Department of Physics at Universität Erlangen-Nürnberg (Germany).

- [1] Yu. S. Kivshar and G.P. Agrawal, *Optical Solitons: From Fibers to Photonic Crystals* (Academic Press, San Diego, 2003).
- [2] G.I. Stegeman, D.N. Christodoulides, and M. Segev, *IEEE J. Sel. Top. Quantum Electron.* **6**, 1419 (2000).
- [3] N.N. Akhmediev and A. Ankiewicz, *Solitons: Nonlinear Pulses and Beams* (Chapman and Hall, London, 1997).
- [4] Y. Silberberg, *Opt. Lett.* **15**, 1282 (1990).
- [5] X. Liu, L.J. Qian, and F.W. Wise, *Phys. Rev. Lett.* **82**, 4631 (1999); X. Liu, K. Beckwitt, and F. Wise, *Phys. Rev. E* **62**, 1328 (2000).
- [6] M. Soljačić, S. Sears, and M. Segev, *Phys. Rev. Lett.* **81**, 4851 (1998); M. Soljačić and M. Segev, *Phys. Rev. E* **62**, 2810 (2000); *Phys. Rev. Lett.* **86**, 420 (2001).
- [7] A.S. Desyatnikov and Yu.S. Kivshar, *Phys. Rev. Lett.* **87**, 033901 (2001).
- [8] G.L. Alfimov, V.M. Eleonsky, N.E. Kulagin, L.M. Lehrmann, and V.P. Silin, *Phys. Lett. A* **138**, 443 (1989).
- [9] D.V. Skryabin, J.M. McSloy, and W.J. Firth, *Phys. Rev. E* **66**, 055602(R) (2002).
- [10] A.S. Desyatnikov and Yu.S. Kivshar, *Phys. Rev. Lett.* **88**, 053901 (2002); *J. Opt. B: Quantum Semiclassical Opt.* **4**, S58 (2002).
- [11] D. Rozas, C.T. Law, and G.A. Schwartzlander, *J. Opt. Soc. Am. B* **14**, 3054 (1997).
- [12] W.J. Firth and D.V. Skryabin, *Phys. Rev. Lett.* **79**, 2450 (1997); D.V. Skryabin and W.J. Firth, *Phys. Rev. E* **58**, 3916 (1998).
- [13] L. Torner and D.V. Petrov, *Electron. Lett.* **33**, 608 (1997); J.P. Torres, J.M. Soto-Crespo, L. Torner, and D.V. Petrov, *J. Opt. Soc. Am. B* **15**, 625 (1998).
- [14] P. Di Trapani, W. Chinaglia, S. Minardi, A. Piskarskas, and G. Valiulis, *Phys. Rev. Lett.* **84**, 3843 (2000).
- [15] Z.H. Musslimani, M. Soljačić, M. Segev, and D.N. Christodoulides, *Phys. Rev. E* **63**, 066608 (2001).
- [16] D. Mihalache, D. Mazilu, I. Towers, B.A. Malomed, and F. Lederer, *J. Opt. A: Pure Appl. Opt.* **4**, 615 (2002).
- [17] D. Mihalache, D. Mazilu, L.-C. Crasovan, B.A. Malomed, and F. Lederer, *Phys. Rev. E* **62**, R1505 (2000).
- [18] D. Mihalache, D. Mazilu, L.-C. Crasovan, I. Towers, A.V. Buryak, B.A. Malomed, L. Torner, J.P. Torres, and F. Lederer, *Phys. Rev. Lett.* **88**, 073902 (2002); D. Mihalache, D. Mazilu, I. Towers, B.A. Malomed, and F. Lederer, *Phys. Rev. E* **67**, 056608 (2003).
- [19] D. Mihalache, D. Mazilu, L.-C. Crasovan, I. Towers, B.A. Malomed, A.V. Buryak, L. Torner, and F. Lederer, *Phys. Rev. E* **66**, 016613 (2002).
- [20] A.G. Vladimirov, J.M. McSloy, D.V. Skryabin, and W.J. Firth, *Phys. Rev. E* **65**, 046606 (2002); D.V. Skryabin and A.G. Vladimirov, *Phys. Rev. Lett.* **89**, 044101 (2002).
- [21] J. Ruostekoski and J.R. Anglin, *Phys. Rev. Lett.* **86**, 3934 (2001); R.A. Battye and P.M. Sutcliffe, *ibid.* **86**, 3989 (2001).
- [22] R.A. Battye, N.R. Cooper, and P.M. Sutcliffe, *Phys. Rev. Lett.* **88**, 080401 (2002).
- [23] J.R. Anglin and W. Ketterle, *Nature (London)* **416**, 211 (2002).
- [24] J.E. Williams and M.J. Holland, *Nature (London)* **401**, 568 (1999).
- [25] M.R. Matthews, B.P. Anderson, P.C. Haljan, D.S. Hall, C.E. Wieman, and E.A. Cornell, *Phys. Rev. Lett.* **83**, 2498 (1999).
- [26] K.W. Madison, F. Chevy, W. Wohlleben, and J. Dalibard, *Phys. Rev. Lett.* **84**, 806 (2000).
- [27] J.R. Abo-Shaeer, C. Raman, J.M. Vogels, and W. Ketterle, *Science* **292**, 476 (2001).
- [28] K.E. Strecker, G.W. Partridge, A.G. Truscott, and R.G. Hulet, *Nature (London)* **417**, 150 (2002); L. Khaykovich, F. Schreck, G. Ferrari, T. Bourdel, J. Cubizolles, L.D. Carr, Y. Castin, and C. Salomon, *Science* **296**, 1290 (2002).
- [29] H. Saito and M. Ueda, *Phys. Rev. Lett.* **90**, 040403 (2003).
- [30] F.Kh. Abdullaev, J.G. Caputo, R.A. Kraenkel, and B.A. Malomed, *Phys. Rev. A* **67**, 013605 (2003).
- [31] P.D. Drummond, *Mod. Phys. Lett. B* **14**, 189 (2000).
- [32] L.-C. Crasovan, G. Molina-Terriza, J.P. Torres, L. Torner, V.M. Pérez-García, and D. Mihalache, *Phys. Rev. E* **66**, 036612 (2002).
- [33] G. Theocharis, D.J. Frantzeskakis, P.G. Kevrekidis, B.A. Malomed, and Yu.S. Kivshar, *Phys. Rev. Lett.* **90**, 120403 (2003).
- [34] L.-C. Crasovan, Y.V. Kartashov, D. Mihalache, L. Torner, Y.S. Kivshar, and V.M. Pérez-García, *Phys. Rev. E* **67**, 046610 (2003).
- [35] V.M. Pérez-García and V. Vekslerchik, *Phys. Rev. E* **67**, 061804 (2003).
- [36] P.S. Julienne, K. Burnett, Y.B. Band, and W.C. Stwalley, *Phys. Rev. A* **58**, R797 (1998).
- [37] D.J. Heinzen, R. Wynar, P.D. Drummond, and K.V. Kheruntsyan, *Phys. Rev. Lett.* **84**, 5029 (2000).
- [38] J. Javanainen and M. Mackie, *Phys. Rev. A* **59**, R3186 (1998).
- [39] L.-M. Duan, A. Sorensen, J.I. Cirac, and P. Zoller, *Phys. Rev. Lett.* **85**, 3991 (2000).
- [40] B.J. Cusack, T.J. Alexander, E.A. Ostrovskaya, and Yu.S. Kivshar, *Phys. Rev. A* **65**, 013609 (2001).
- [41] S.J.J.M.F. Kokkelmans and M.J. Holland, *Phys. Rev. Lett.* **89**, 180401 (2002).
- [42] R. Wynar, R.S. Freeland, D.J. Han, C. Ryu, and D.J. Heinzen, *Science* **287**, 1016 (2000).
- [43] E.A. Donley, N.R. Claussen, S.T. Thompson, and C.E. Wieman, *Nature (London)* **417**, 529 (2002).
- [44] L. Torner, J.P. Torres, D.V. Petrov, and J.M. Soto-Crespo, *Opt. Quantum Electron.* **30**, 89 (1998).
- [45] D.V. Petrov, L. Torner, J. Martorell, R. Vilaseca, J.P. Torres, and C. Cojocar, *Opt. Lett.* **23**, 1444 (1998).
- [46] S. Minardi, G. Molina-Terriza, P. Di Trapani, J.P. Torres, and L. Torner, *Opt. Lett.* **26**, 1004 (2001).
- [47] Y.V. Kartashov, G. Molina-Terriza, and L. Torner, *J. Opt. Soc. Am. B* **19**, 2682 (2002).
- [48] Y.V. Kartashov, L.-C. Crasovan, D. Mihalache, and L. Torner, *Phys. Rev. Lett.* **89**, 273902 (2002).
- [49] I. Towers, A.V. Buryak, R.A. Sammut, and B.A. Malomed, *Phys. Rev. E* **63**, 055601(R) (2001).
- [50] M. Quiroga-Teixeiro and H. Michinel, *J. Opt. Soc. Am. B* **14**, 2004 (1997); H. Michinel, J. Campo-Táboas, M.L. Quiroga-Teixeiro, J.R. Salgueiro, and R. García-Fernández, *J. Opt. B: Quantum Semiclassical Opt.* **3**, 314 (2001).
- [51] V.I. Berezghiani, V. Skarka, and N.B. Aleksić, *Phys. Rev. E* **64**, 057601 (2001).
- [52] I. Towers, A.V. Buryak, R.A. Sammut, B.A. Malomed, L.-C. Crasovan, and D. Mihalache, *Phys. Lett. A* **288**, 292 (2001).
- [53] R.L. Pego and H.A. Warchall, *J. Nonlinear Sci.* **12**, 347 (2002).
- [54] B.A. Malomed, L.-C. Crasovan, and D. Mihalache, *Physica D*

- 161**, 187 (2002); D. Mihalache, D. Mazilu, L.-C. Crasovan, B.A. Malomed, and F. Lederer, *Phys. Rev. E* **61**, 7142 (2000).
- [55] F. Smektala, C. Quemard, V. Couderc, and A. Barthélémy, *J. Non-Cryst. Solids* **274**, 232 (2000); C. Zhan, D. Zhang, D. Zhu, D. Wang, Y. Li, D. Li, Z. Lu, L. Zhao, and Y. Nie, *J. Opt. Soc. Am. B* **19**, 369 (2002); G. Boudebs, S. Cherukulappurath, H. Leblond, J. Troles, F. Smektala, and F. Sanchez, *Opt. Commun.* **219**, 427 (2003).
- [56] E.M. Wright, B.L. Lawrence, W. Torruellas, and G. Stegeman, *Opt. Lett.* **20**, 2481 (1995); S. Gatz and J. Herrmann, *IEEE J. Quantum Electron.* **QE-28**, 1732 (1992); R.H. Enns, S.S. Rangnekar, and A.E. Kaplan, *Phys. Rev. A* **35**, 466 (1987); D. Mihalache, D. Mazilu, M. Bertolotti, and C. Sabilia, *J. Opt. Soc. Am. B* **5**, 565 (1988).
- [57] A. Desyatnikov, A. Maimistov, and B. Malomed, *Phys. Rev. E* **61**, 3107 (2000).
- [58] B.A. Malomed, *Phys. Rev. E* **58**, 7928 (1998).